Moesin Is a Major Regulator of Centrosome Behavior in Epithelial Cells with Extra Centrosomes

Dora Sabino, Delphine Gogendeau, Davide Gambarotto, Maddalena Nano, Carole Pennetier, Florent Dingli, Guillaume Arras, Damarys Loew, Renata Basto

Article

Current Biology

Moesin Is a Major Regulator of Centrosome Behavior in Epithelial Cells with Extra Centrosomes

Graphical Abstract

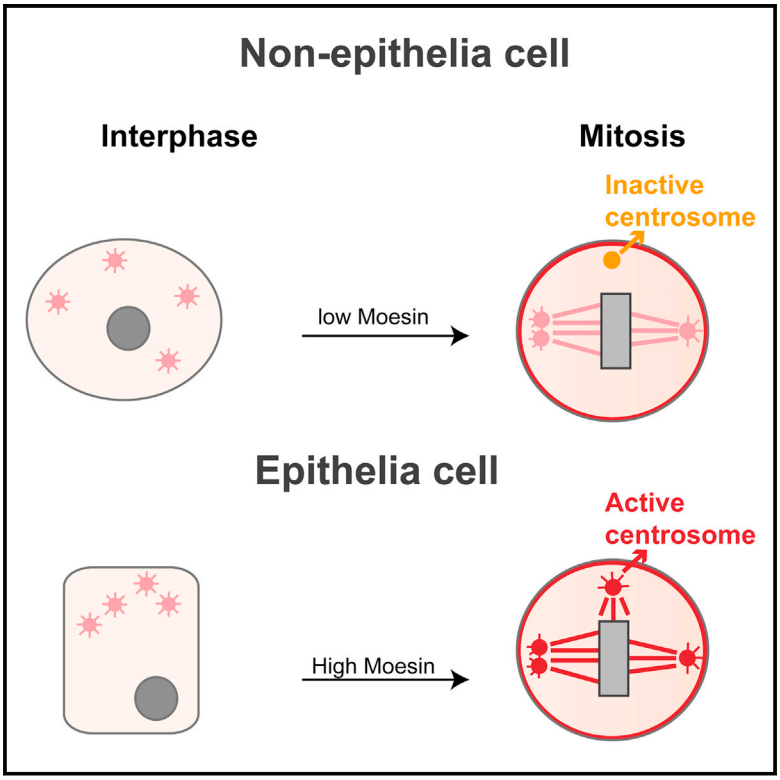

Authors

Dora Sabino, Delphine Gogendeau, ..., Damarys Loew, Renata Basto

Correspondence

renata.basto@curie.fr

In Brief

Sabino et al. study the consequences of centrosome amplification in an epithelium. They find that mechanisms of extra-centrosome clustering and inactivation are not fully efficient. High levels of Moesin, an ERM protein, contribute to a failure in bipolar spindle assembly leading to aneuploidy and priming tumor-initiating events.

Highlights

- Consequences of centrosome amplification in epithelia are discussed
- Centrosome clustering or inactivation is not fully efficient
- High levels of Moesin contribute to defects in bipolar spindle assembly
- Centrosome amplification generates aneuploidy and epithelial transformation

Sabino et al., 2015, Current Biology *25*, 879–889
March 30, 2015
http://dx.doi.org/10.1016/j.cub.2015.01.066

CellPress

Current Biology
Article

Moesin Is a Major Regulator of Centrosome Behavior in Epithelial Cells with Extra Centrosomes

Dora Sabino,[1,3] Delphine Gogendeau,[1] Davide Gambarotto,[1] Maddalena Nano,[1] Carole Pennetier,[1] Florent Dingli,[2] Guillaume Arras,[2] Damarys Loew,[2] and Renata Basto[1,*]
[1]Institut Curie, CNRS UMR144, 12 Rue Lhomond, 75005 Paris, France
[2]Institut Curie, CNRS, LSMP, 26 Rue d'Ulm, 75005 Paris, France
[3]Present address: Gustave Roussy, UMR8126, 94805 Villejuif Cedex, France
*Correspondence: renata.basto@curie.fr
http://dx.doi.org/10.1016/j.cub.2015.01.066

SUMMARY

Centrosome amplification has severe consequences during development and is thought to contribute to a variety of diseases such as cancer and microcephaly. However, the adverse effects of centrosome amplification in epithelia are still not known. Here, we investigate the consequences of centrosome amplification in the *Drosophila* wing disc epithelium. We found that epithelial cells exhibit mechanisms of clustering but also inactivation of extra centrosomes. Importantly, these mechanisms are not fully efficient, and both aneuploidy and cell death can be detected. Epithelial cells with extra centrosomes generate tumors when transplanted into WT hosts and inhibition of cell death results in tissue over-growth and disorganization. Using SILAC-fly, we found that Moesin, a FERM domain protein, is specifically upregulated in wing discs with extra centrosomes. Moesin localizes to the centrosomes and mitotic spindle during mitosis, and we show that Moesin upregulation influences extra-centrosome behavior and robust bipolar spindle formation. This study provides a mechanistic explanation for the increased aneuploidy and transformation potential primed by centrosome amplification in epithelial tissues.

INTRODUCTION

Centrosomes are the main microtubule (MT) organizing centers in animal cells [1] and are composed of a pair of centrioles surrounded by pericentriolar material (PCM) [2]. Centrosome amplification (more than two centrosomes per cell) is commonly found in cancers [3, 4] and is accompanied of genomic instabilities, including aneuploidy. To avoid the generation of multipolar mitosis and consequently high levels of aneuploidy, mechanisms of centrosome clustering are in place, both in vivo and in cell lines [5–9] highlighting the high selective pressure to acquire bipolarity during mitosis. Sak/Plk4 kinase is the master regulator of centriole duplication [10, 11], and its overexpression leads to centrosome amplification [12].

The mounting insights coming from mouse and *Drosophila* studies have showed that the consequences of centrosome amplification are highly dependent on tissue-specific contexts. Centrosome amplification in *Drosophila* larval brain neuroblasts generates tumors due to stem cell pool expansion, however and remarkably, in the absence of aneuploidy [6]. On the other hand, mice with brain-driven centrosome amplification have no tumors and showed microcephaly [9].

Investigating the consequences of centrosome amplification in epithelial cells is of particular interest since most cancers are of epithelial origin [13]. To do so, we characterized the wing disc in *Drosophila* upon Sak overexpression (*Sak*OE). We found that centrosome amplification causes aneuploidy leading to tumor formation in transplantation assays. To understand the differential response to centrosome amplification between wing discs and brains, we performed comparative in vivo SILAC and identified Moesin as a regulator of centrosome behavior in epithelial cells.

RESULTS

Sak Overexpression in the Wing Disc Causes Centrosome Amplification

We analyzed the overexpression of *Sak* (here referred to as *SakOE*) in the fly wing disc (Figure 1A), using the previously described line [6] that expresses the centriole duplication kinase Sak under a moderate ubiquitous promoter [14]. We analyzed cells exclusively from the wing pouch region (Figure 1A), a highly proliferative region during larval stages [15]. Centrosomes were analyzed by the co-localization of the centriolar and PCM marker Pericentrin like protein (Plp) [16] with the PCM marker Centrosomin (Cnn). Mitotic cells showed a variable number of supernumerary centrosomes in 19% of the cells (Figure 1D). Importantly, wild-type (WT) wing disc cells never showed extra centrosomes (Figures 1B–1D). We conclude that wing disc epithelial cells can generate extra centrosomes in response to Sak overexpression [6].

Mechanisms of Extra-centrosome Clustering and Inactivation Are Present but Are Not Fully Efficient in the Wing Disc

During the characterization of *SakOE* discs, we observed that, at metaphase, most cells with centrosome amplification formed bipolar spindles (Figures 1B and 1C). We analyzed cell division using time-lapse microscopy in wing discs expressing different transgene combinations (Figures 1E and 1F). In WT discs, two centrosomes formed a bipolar spindle (Figure 1E). After

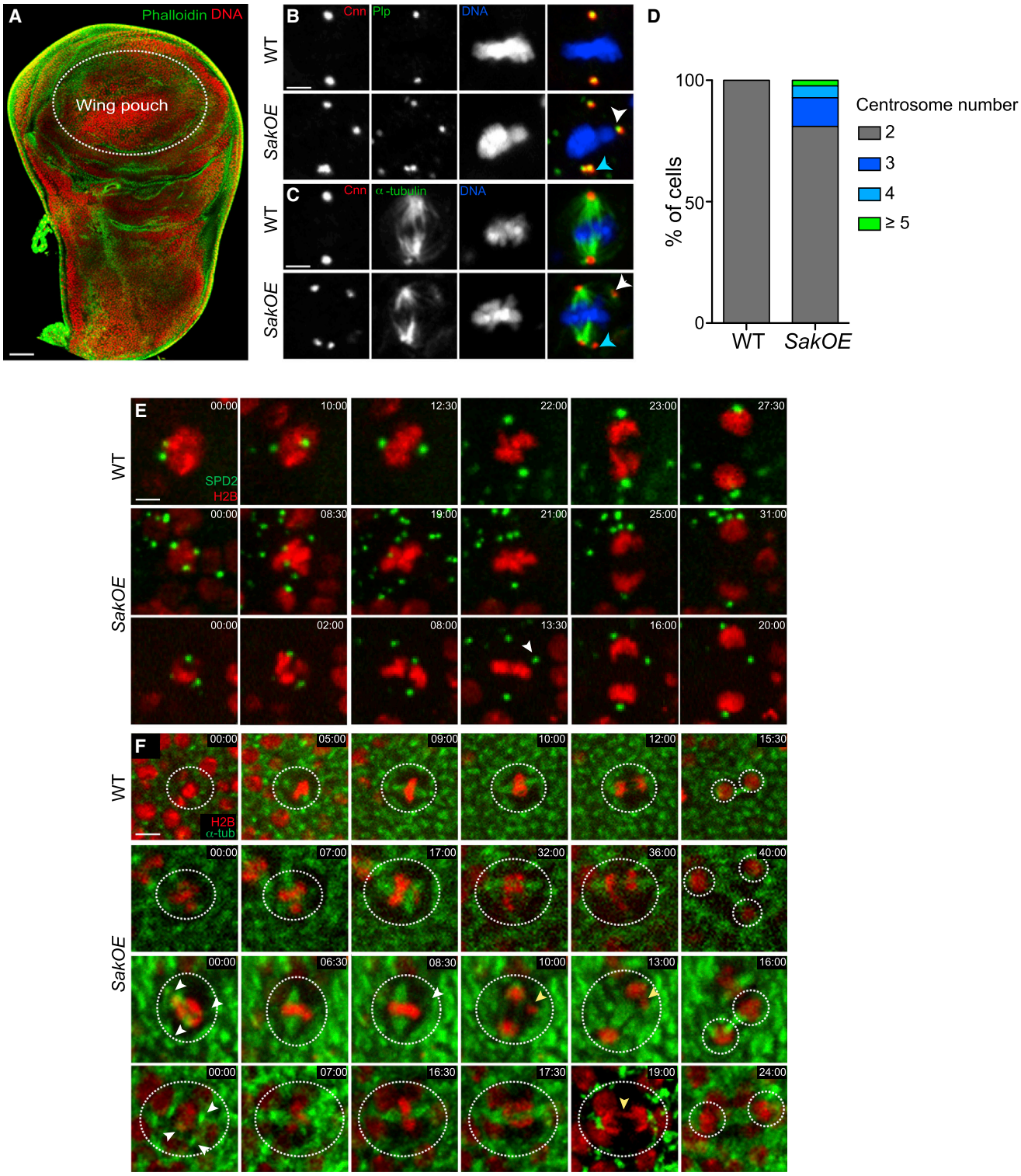

Figure 1. Analysis of Wing Disc Epithelia with Extra Centrosomes

(A) Phalloidin (green) and DNA (red) staining of a WT third instar wing disc (WD). The dashed line labels the wing pouch, a highly proliferative region at this developmental stage. Scale bar, 100 μm.

(B and C) Pictures of WT and *SakOE* WD cells stained with Cnn to label PCM (left and showed in red in the merged panel) and Plp (B) or α-tubulin (C) to label both centrioles and PCM (B) or MTs (middle, showed in green in the merged panel) antibodies. DNA is shown in blue. White arrowheads labels un-clustered centrosomes and blue arrowheads label clustered centrosomes at the spindle poles. Scale bar, 5 μm.

(D) Graph bars showing the quantification of centrosome numbers in WT (n = 110) and *SakOE* WD cells (n = 166).

(legend continued on next page)

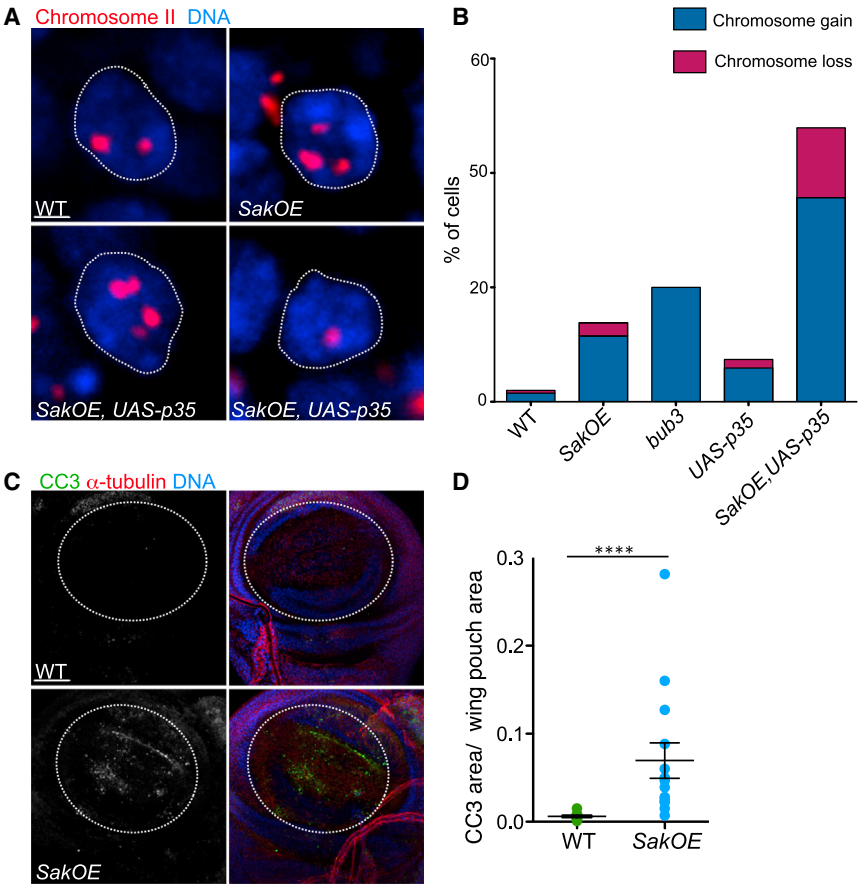

Figure 2. Aneuploidy and Cell Death by Apoptosis in the Wing Disc Epithelia with Extra Centrosomes

(A) Projections of WD nuclei showing FISH staining using probes for chromosome II (showed in red) in WT, *SakOE*, and *UAS-p35;SakOE* (n = 180, n = 570 and n = 490 WD cells, respectively). DNA is shown in blue. Scale bar, 4 μm.

(B) Graph bars showing the quantification of FISH signals for chromosome gain (dark blue) and chromosome loss (dark pink) of the indicated genotypes (see the Experimental Procedures for a comprehensive description of FISH quantification).

(C) Pictures of WT (left) and *SakOE* (right) WDs stained with cleaved caspase 3 (CC3) to label apoptotic cells (shown in green) and α-tubulin (shown in red) antibodies. DNA is shown in blue. Scale bar, 100 μm.

(D) A dot-plot chart showing the quantification of the ratio between CC3 positive area and the WD area in WT and *SakOE* (n = 8 and n = 10 WDs, respectively). The line represents the mean, and the error bars represent the SD. Statistical significance (SS) was assessed by an unpaired Student's t test, ****$p < 0.0001$.

See also Figure S1.

anaphase and cytokinesis, both daughter nuclei move toward the basal side (data not shown). In *SakOE* discs, the great majority of cells with supernumerary centrosomes formed bipolar spindles by metaphase. The major mechanism contributing to bipolar spindle formation was inactivation, defined as the gradual loss of microtubule-nucleating capacity noticed in more than half of the cells (57.5%, n = 23 out of 40 cells) (Figure 1E, bottom panel) with extra centrosomes. In addition, centrosome clustering was also present (32.5%, n = 13 out of 40 cells) (Figure 1E, middle panel). Centrosome inactivation was already described in neuroblasts, but in these cells this mechanism was less frequent [6]. Importantly, tripolar divisions, where extra centrosomes remained un-clustered and active centrosomes were also noticed (10%, n = 4 out of 40 cells) (Figure 1F, second panel). In addition, lagging chromosomes were detected in 25% (n = 10 out of 40 cells) of *SakOE* cells dividing bipolarly (Figure 1F, third and fourth panel, and Figure 7A). Although we do not have the resolution to detect merotelic attachments, these most likely result from transient multipolar states during prometaphase as shown in tissue culture [7, 17].

We conclude that, unlike the brain, where all *SakOE* cells divided in a bipolar way without chromosome mis-segregation [6], wing disc cells show abnormal cell division in response to centrosome amplification.

Aneuploidy and Not Spindle Positioning Defects Contribute to Apoptotic Cell Death in *Sak*OE Wing Discs

Abnormal cell division generates aneuploid cells with unequal chromosome content [18]. To ascertain the levels of aneuploidy in *SakOE* epithelia, we used fluorescent in situ hybridization (FISH) and used WT and SAC *bub3* mutant [19, 20] wing discs as negative and positive controls, respectively (Figure 2A; results not shown). Using a probe for chromosome II, we found that 13.7% of *SakOE* wing disc cells (n = 570 cells from three wing discs) were aneuploid. Of these, 9.5% contained at least one extra chromosome, while chromosome loss was less frequent (2.3%) (Figures 2A and 2B). *Drosophila* cells contain only four chromosomes, and loss of one single chromosome might be quite deleterious. Several studies have shown that aneuploid cells are frequently not tolerated and removed from the

(E) Stills of time-lapse movies of mitotic WT (top) and *SakOE* (middle and bottom) WD cells expressing histone-RFP to label chromosomes (shown in red) and Spd2-GFP to label the centrosomes (shown in green). The dashed circles surround each cell. In the *SakOE* cell (middle panel) extra centrosomes cluster at the spindle poles, while, in the *SakOE* cell shown in the bottom, the extra centrosome remain in the cytoplasm (white arrowhead). Time is in minutes. Scale bar, 10 μm.

(F) Stills of time-lapse movies of mitotic WT (top) and *SakOE* (middle and bottom) WD cells expressing histone-RFP to label chromosomes (shown in red) and α-tubulin-GFP to label the spindle (shown in green). The dashed circles surround each cell. The *SakOE* cell (second panel) divides in three cells. In the third and fourth panels, three centrosomes can be noticed (white arrowheads), which cause chromosome mis-segregation and lagging chromosomes (yellow arrowhead). Time is in minutes. Scale bar, 10 μm.

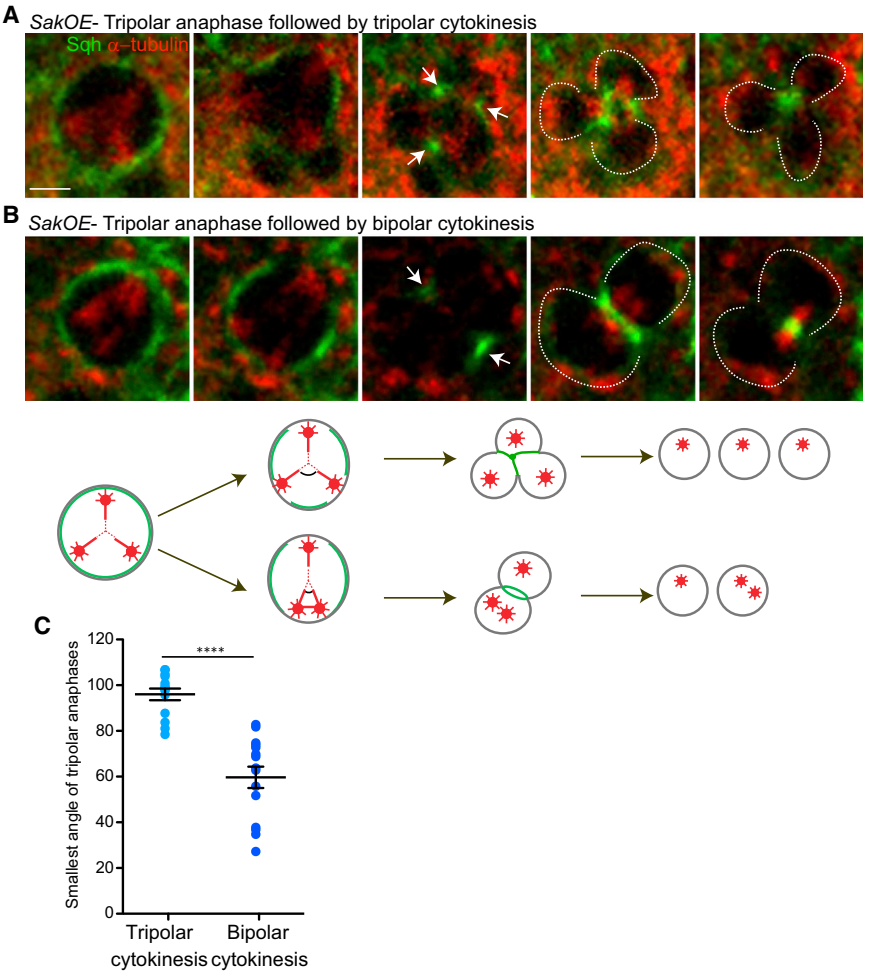

Figure 3. Analysis of Cytokinesis in *SakOE* Wing Disc Cells

(A and B) Stills of time-lapse movies of *SakOE* WDs cells expressing Sqh-GFP (shown in green) and α-tubulin-RFP (shown in red). Cells undergo tripolar anaphases with tripolar (A) or bipolar cytokinesis (B) can be detected. The white arrows point at Myo-II accumulation at the cortex, and the dashed circles surround the daughter cells. Scale bar, 5 μm

(C) A dot-plot chart showing the quantification of the smallest angle formed in tripolar divisions at the point of intersection of the three MT arrays. The line represents the mean and the error bars the SD. SS was assessed by an unpaired Student's t test, ****$p < 0.001$.

population of cycling cells by apoptosis [7, 9, 21–23]. In the wing disc, aneuploid cells undergo apoptosis and are removed by delamination through the basal surface [24]. Measurements of the positive area for the cleaved caspase 3 (CC3) apoptotic marker revealed that *Sak*OE discs showed higher levels of cell death (Figures 2C and 2D) when compared to WT.

To ascertain whether the apoptosis plays a role in eliminating aneuploid cells, we blocked cell death using a transgene that expresses the baculovirus caspase inhibitor p35 (*UAS-p35*) under the control of the Actin5C-Gal4 promoter (Act-G4). Even if aneuploidy could also be detected in *UAS-p35*, *Act-G4 discs*, when combined with *SakOE* wing discs a considerable increase in the frequency of cells with both chromosome gains and losses were detected (35.7% chromosome gain and 12.2% chromosome loss, n = 490 cells from three discs) (Figure 2B). We concluded that apoptosis plays a major role inhibiting the accumulation of aneuploid cells in the wing disc.

Since defects in planar spindle alignment have been shown to cause apoptotic cell death and delamination in wing disc epithelia [25–27], and *SakOE* neuroblasts also showed spindle mispositioning [6], we analyzed spindle positioning by measuring the angle formed between the main axis of the spindle and the apical surface (Figure S1A). We observed that 68.0% of *SakOE* prometaphase cells showed clear defects in spindle positioning (angle $\geq 15^{\circ}$). However, by metaphase and anaphase the large majority of cells (90.0% and 91% of the cells) presented planar spindle orientation or only small deviations (Figures S1A and S1B). We concluded that, even if both spindle positioning defects and aneuploidy contribute to cell death by apoptosis in *SakOE* discs, the major contribution most probably results from chromosome segregation defects.

Extra-centrosomal Tripolar Anaphases Can Be Resolved into Bipolar Cytokinesis

To further characterize the outcome of tripolar divisions, we extended the time-lapse analysis to tripolar mitosis using the regulatory myosin-II (myo-II) light chain (spaghetti squash) to characterize cytokinesis. We observed that ~60% of tripolar anaphases (25 out of 40 tripolar divisions) resolved in bipolar cytokinesis (Figure 3B), while the remaining 40% (15 out of 40 cells) completed division with tripolar cytokinesis. Furthermore, we observed a correlation between the number of daughter cells (two or three) and the distribution of myo-II at the cortex by anaphase in two or three distinct regions, respectively (Figures 3A and 3B). Interestingly in tripolar mitosis, a robust MT array resembling a triangle can be noticed (Figures 3A and 3B). Measurement of the angle at the point of intersection showed a bias toward tripolar cytokinesis, when superior to 90° (Figure 3C). Astral MTs inhibit myo-II accumulation at the cortex [28]. Likely, a tripolar anaphase with poles quite far apart results in the maintenance of three cortical myo-II regions (Figure 3A), which leads to tripolar cytokinesis. On the contrary, if two of the poles are close enough, myo-II might just accumulate in two opposite regions, similarly to a true bipolar spindle. Interestingly, trisomies due to multipolar mitosis coupled to incomplete cytokinesis were reported in Wilms' tumors [29].

Centrosome Amplification Drives Tumorigenesis in Epithelial Tissues

We then investigated whether *SakOE* epithelial cells would have the potential to become over-proliferative in transplantation

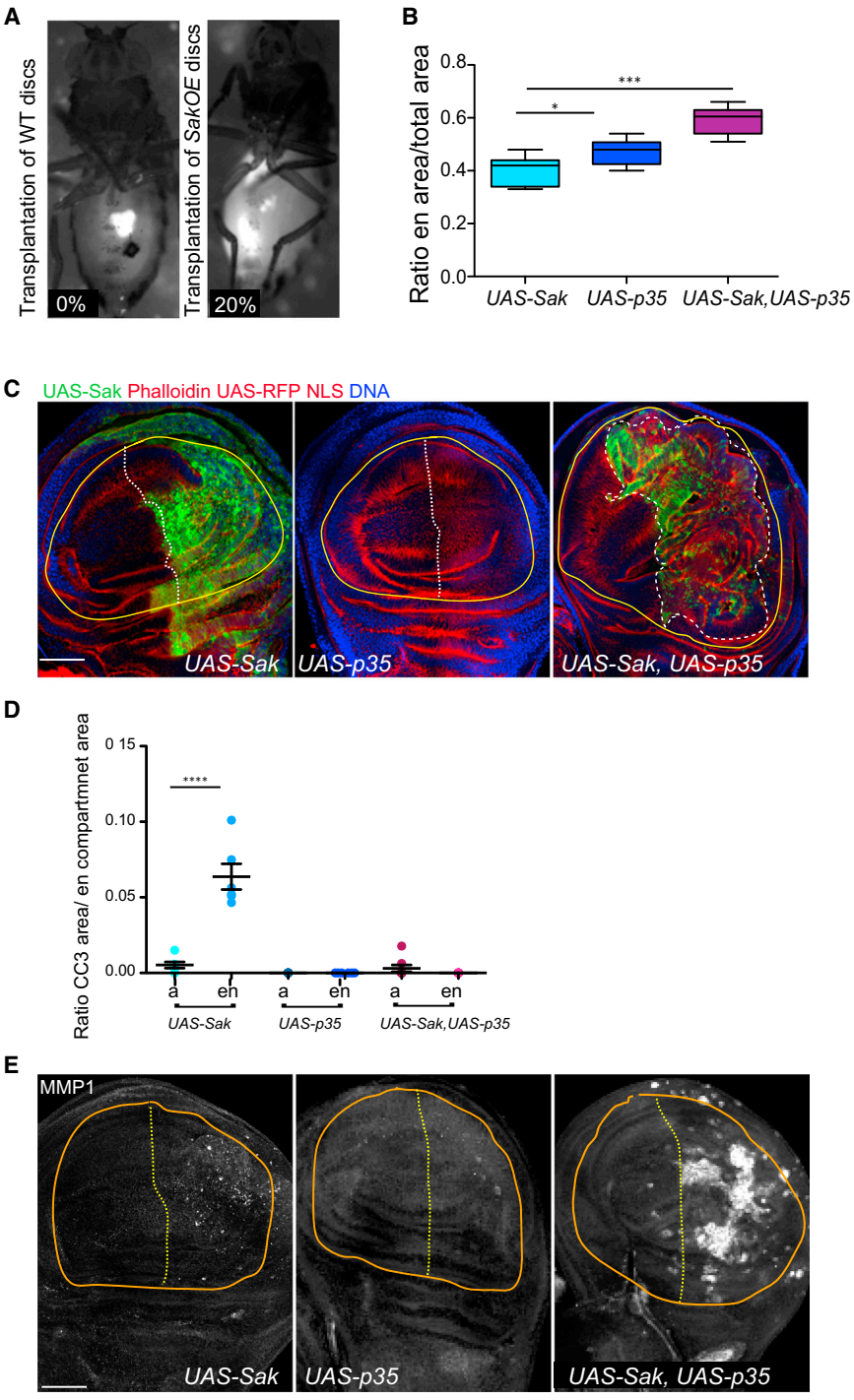

Figure 4. Centrosome Amplification Causes Tumor Formation in the Wing Disc Epithelia

(A) Pictures of WT adult host flies transplanted with tubulin-GFP (left) or tubulin-GFP, *SakOE* (right) pieces of L3 WDs.

(B) A box chart showing the quantification of the ration between the en compartment and total wing pouch area in *UAS-Sak*, *UAS-p35*, and *UAS-Sak,UAS-p35* (n = 8, n = 7, and n = 10 WDs, respectively). The line represents the mean and the error bars the SD. SS was assessed by a Mann-Whitney test, *p < 0.05 and ***p < 0.001.

(C) Pictures of WDs expressing *UAS-Sak* (left), *UAS-p35* (middle), and *UAS-Sak,UAS-p35* (right) transgenic under the control of enGAl4-NLS RFP and stained with phalloidin to label actin (shown in red). Green shows the expression of *UAS-Sak*, and DNA is shown in blue. The dashed white line marks the border between the en compartment (to the right), and the yellow line marks the wing pouch. Scale bar, 100 μm.

(D) A dot-plot chart of the ratio between the CC3 area and the WD area in compartment of the indicated genotypes in the anterior (a) used as a control and the en posterior compartments (n = 6 WDs for *UAS-Sak* and *UAS-p35* and n = 8 WDs for *UAS-Sak,UAS-p35)*. The line represents the mean, and the error bars represent the SD. SS was assessed by an unpaired Student's t test, ****p < 0.001.

(E) Pictures of the basal side of epithelial WDs expressing the indicated transgenes under the control of enGAl4 stained with MMP1 to label basement membrane degradation. The white dashed line delimits the en compartment, and the orange line surrounds the wing pouch region. Scale bar, 100 μm.

assays previously described [6, 24, 30–32]. Twenty percent (eight out of 40 hosts) (Figure 4A) of the transplanted healthy hosts developed tumors and died prematurely, which was not the case upon transplantations of WT discs (zero out of 40 hosts).

We next inhibited cell death using *UAS-p35* together with a transgene of *UAS-Sak* and expressed it specifically in the wing disc posterior compartment using the engrailed (en)-Gal4 promoter. In this case, anterior cells, which do not express the en promoter, function as an internal control. UAS-*Sak*,en>Gal4 discs showed disorganization associated with cell death (Figures 4C, left panel, and Figure 4D), while *UAS-p35, en>Gal4* (Figures 4C, middle panel, and Figure 4D) did not cause any obvious defect. When apoptosis was inhibited (*UAS-Sak, UAS-p35*, *en>Gal4*) (Figure 4D), tissue disorganization (Figure 4C, right panel) was noticed accompanied by enlargement of the compartment that appeared severely deformed (Figure 4B). Furthermore, the levels of the Matrix metalloproteinase 1 (MMP1) [33] (Figure 4E) were elevated at the basal side of the epithelium showing that, similarly to checkpoint aneuploid mutants, inhibition of apoptosis leads to the activation of MMP1 expression [24].

Altogether, our in vivo analysis indicates that centrosome amplification represents a tumorigenic event in the fly epithelium.

Increased Moesin Levels Correlate with Inefficient Centrosome Inactivation in Epithelial Cells

The results presented so far clearly point to intrinsic differences related with extra-centrosome behavior between epithelial and

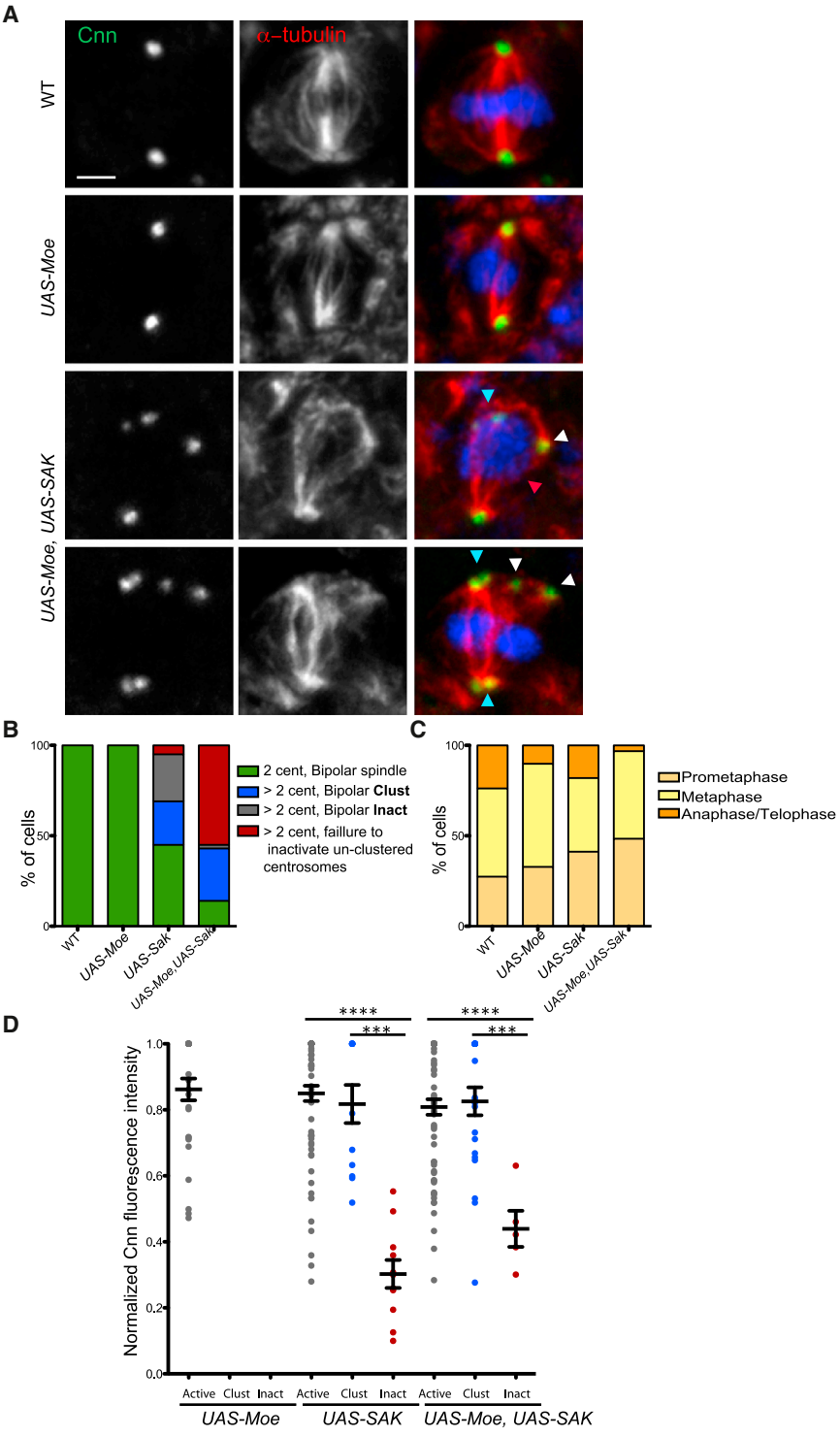

Figure 5. Increased Moesin Levels Lead to Maintenance of Active Un-clustered Centrosomes

(A) Pictures of WT, *UAS-MoeOE*, and *UAS-MoeOE, UAS-SakOE* wing disc cells stained with Cnn (left, shown in green in the merged panel) and α-tubulin antibodies (middle, shown in red in the merged panel). DNA is shown in blue. Blue and white arrowheads point at clustered and active centrosomes, respectively. Scale bar, 5 μm.

(B and C) Graph bars showing the quantification of spindle morphology and the distribution of mitotic phases in *UAS-MoeOE* (n = 33 cells from three WDs), *UAS-Sak* (n = 101 cells from six WD), and *UAS-MoeOE, UAS-Sak* (n = 93 cells from eight WDs).

(D) A dot-plot chart showing the quantification of normalized Cnn fluorescence intensity in *UAS-Moe*, *UAS-Sak*, and *UAS-MoeOE, UAS-Sak* (n = 29, n = 93, and n = 95 WD cells, respectively, from at least four different discs). The line represents the mean, and the error bars represent the SD. SS was assessed by an unpaired Student's t test, ***p < 0.001 and ****p < 0.0001.

See also Figures S2 and S3.

non-epithelial cells (neuroblasts). To identify molecular differences in cells with extra centrosomes, we developed a stable isotope labeling by amino acids in cell culture (SILAC) in flies (SILAC-fly) to quantitatively analyze by mass spectrometry (MS)-based proteomics, protein levels in different tissues. We compared WT and *SakOE* wing discs and brains (Figure S2A). We obtained a list of seven candidates that were specifically upregulated in *SakOE* wing discs (Figure S2B). Of these putative candidates, there was only a known cytoskeleton protein, the FERM domain ERM family member Moesin (Moe). Moe is plays important functions in cortical rigidity, cytoskeleton organization, and spindle morphogenesis [34, 35].

Analysis of wing disc extracts by western blot confirmed a 4-fold upregulation of endogenous Moe specifically in *Sak*OE wing disc extracts, but not in brain extracts (Figure S2C).

To test whether genetic modulation of Moe levels could impact on the behavior of supernumerary centrosomes, we analyzed Moe overexpression (*MoeOE*) using the UAS-Gal4 system with Act-G4. We also induced Sak overexpression using the *UAS-Sak* transgene (*UAS-Sak)* to obtain higher levels of centrosome amplification (Figure S3) and similarly to *SakOE* discs, the major mechanism that promoted bipolar spindle formation was centrosome inactivation. Importantly, the proportion of abnormal spindles was fairly equivalent (Figure 6B). *MoeOE* did not cause centrosome amplification or defects in bipolar spindle formation. However, mitotic progression was delayed, probably due to lack of spindle planarity and consequent delay in establishing correct kinetochore-MT attachment (Figures 5A–5C; data not shown).

UAS-MoeOE,UAS-Sak discs showed an aggravated phenotype when compared to *SakOE* or *UAS-Sak* discs. Although in

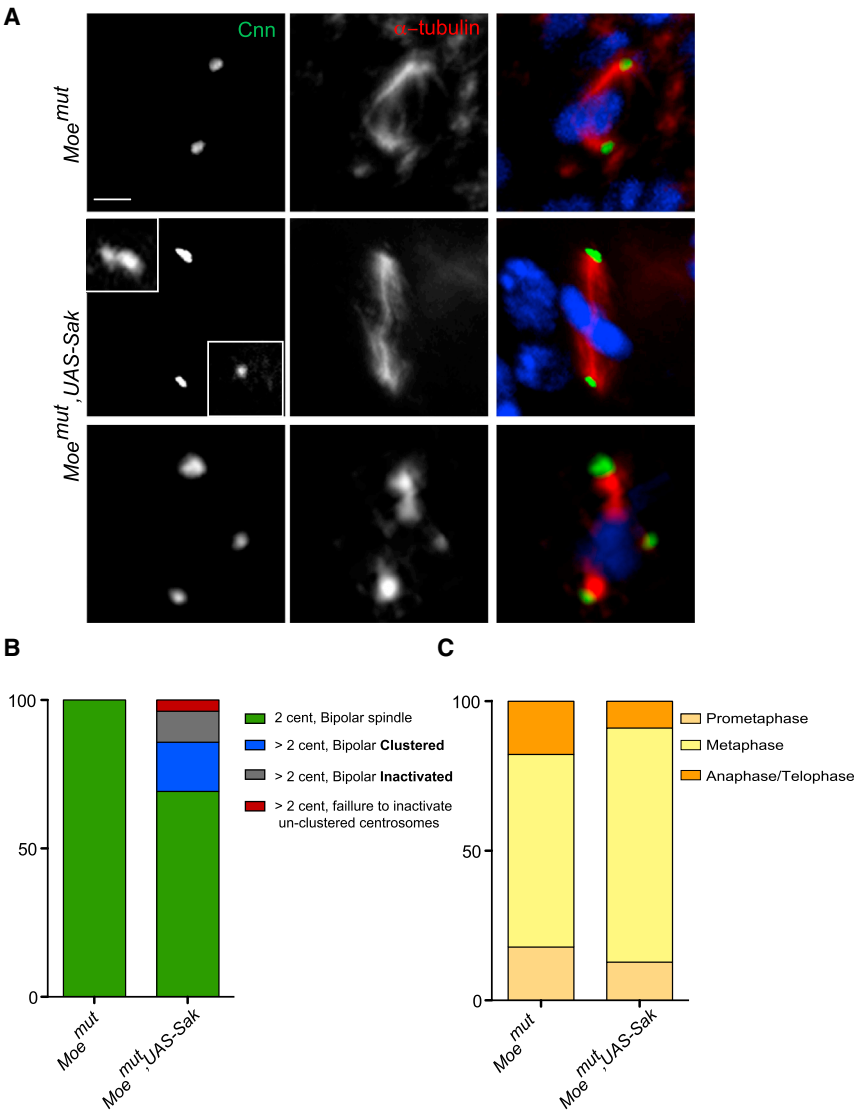

Figure 6. Characterization of *Moe*^{mut}*,UAS-Sak* Wing Discs

(A) Pictures of *Moe*^{mut} and *Moe*^{mut}*,UAS-Sak* mutant cells stained with Cnn (shown in green) and α-tubulin (shown in red). DNA is shown in blue. Scale bar, 5 μm (B and C) Graph bars showing the quantification of spindle morphology and the distribution of mitotic phases in *Moe*^{mut} (n = 45 cells, from four WDs) and *Moe*^{mut}*, UAS-Sak* (n = 78 cells, from five WDs) mutants.

See also Figure S4.

cells that contained extra centrosomes, clustering still occurred (Figure 5A, blue arrowheads), in 55% of the cells, un-clustered centrosomes remained active and nucleated robust MT bundles that contacted the DNA (Figures 5A and 5B, white arrowhead). Un-clustered centrosomes seemed to be maintained in an active status, as assessed by a strong MT nucleation foci (Figures 5A, white arrowheads, and 5B). Moreover, we also observed an increase in the percentage of cells in prometaphase and anaphases were only rarely seen (Figure 5C). Importantly, the percentage of cells that contained extra centrosomes was overall increased in *UAS-MoeOE,UAS-Sak* discs. Due to mitotic abnormalities, it is also possible that these cells failed cytokinesis, which will contribute to increase overall centrosome numbers.

We next quantified Cnn levels (see the Supplemental Experimental Procedures) at the centrosomes. We classified centrosomes as active (two main centrosomes of a mitotic spindle and un-clustered centrosomes localized in the cytoplasm that displayed robust MT nucleation foci), clustered (when two centrosomes could be identified at a spindle pole), and inactive (when a centrosome was not localized at the spindle pole and did not display a robust MT nucleation foci). We normalized Cnn levels in each cell (see the Experimental Procedures). We found that even if Cnn levels were quite variable inactive centrosomes contained reduced Cnn levels (Figure 5D) when compared to active ones. Importantly, in cells with high Moe levels, the increase in the percentage of active un-clustered centrosomes resulted from increased Cnn at the centrosome. Importantly, Moe overexpression in *UAS-Sak* brains did not influence spindle formation or mitotic progression (data not shown), suggesting once more a tissue-specific response.

Altogether our results show that increased Moe levels influence spindle assembly and function exclusively in epithelial cells that contain extra centrosomes.

To test whether decreasing Moe levels promoted bipolar spindle formation in the presence of extra centrosomes, we combined centrosome amplification (induced by *UAS-SAK* combined with Act-G4) with *Moe* mutations (*Moe*^{mut}). These discs were highly abnormal displaying several folds, and the tissue appeared highly disorganized. Most mitotic spindles were non-planar, and we observed high levels of cell death (data not shown). The majority of *Moe*^{mut}*,UAS-Sak* cells with extra centrosomes presented bipolar configurations (Figures 6A and 6B). Importantly, both clustering and inactivation seemed to improve. Concerning clustering, extra centrosomes appeared extremely close to each other in these cells (see inset in Figure 6A). In addition, in cells where we could clearly identify un-clustered centrosomes (Figure 6A), these appeared inactive (Figures 6A and 6B). Analysis of *Moe*^{mut}*,UAS-Sak* cells showed an improvement when compared to *UAS-Moe, UAS-SAK*, although a clear delay in mitotic progression was still present (Figures 5C and 6C).

Moesin Localizes to the Spindle and Centrosomes during Mitosis

Since cortical rigidity plays an important role in mitotic spindle assembly [36], we investigated whether Moe cortical

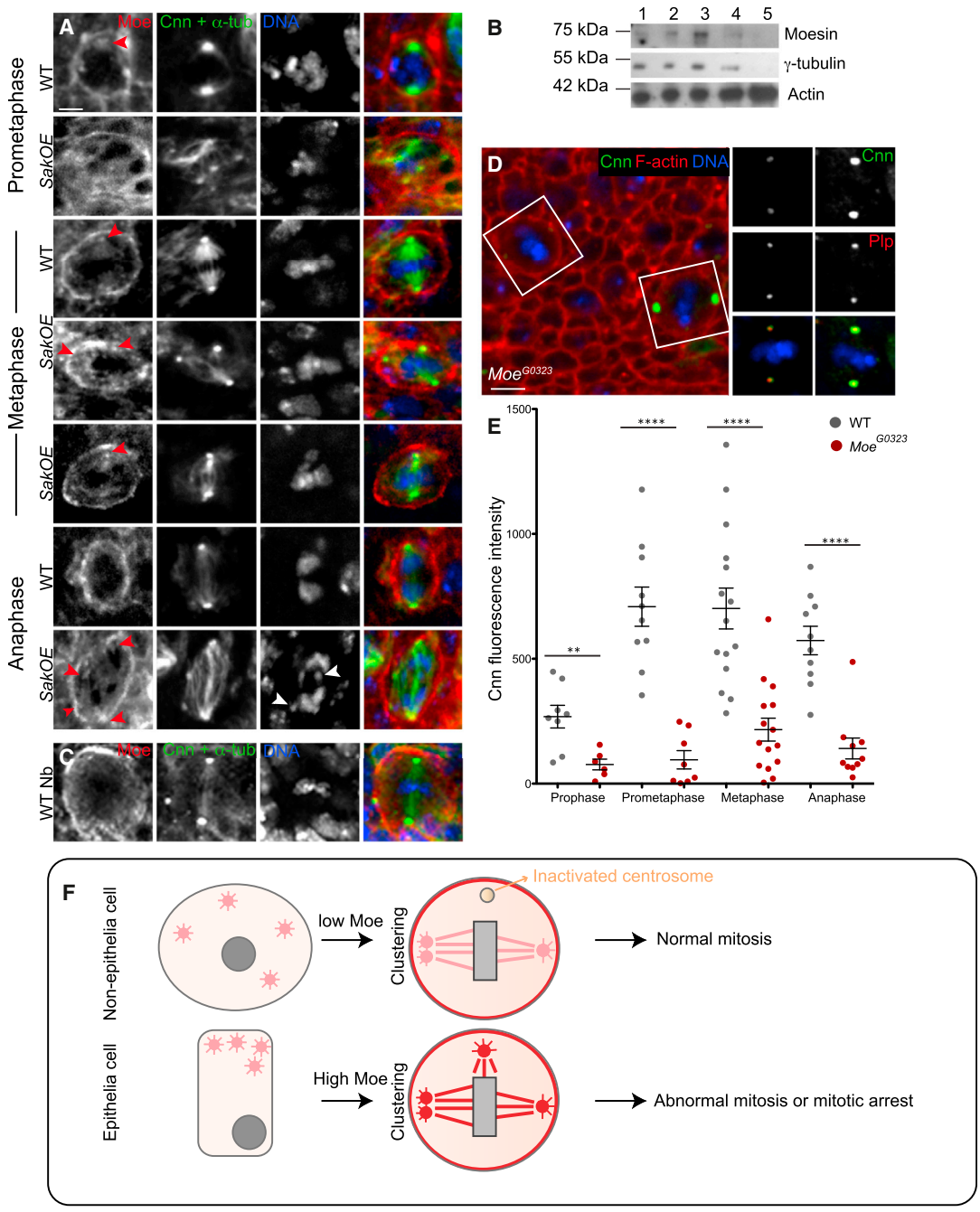

Figure 7. Moesin Localizes to the Centrosome in Mitotic Wing Disc Cells

(A) Pictures of WT and *SakOE* WD cells stained with Moe (left, shown in red in the merged panel), Cnn, and α-tubulin (middle, shown in green the merged panel) antibodies. DNA is shown in blue. Red arrowheads show Moe at active un-clustered centrosomes. Scale bar, 5 μm

(B) Western blot of centrosome purification fractions probed with antibodies against Moesin, γ-tubulin, and actin.

(C) Picture of a WT neuroblast stained as in (A). Scale bar, 10 μm

(D) On the left, low-magnification picture of Moe^{G0323} mutant WD showing Cnn (in green) antibodies and phalloidin (in red). On the right, higher magnification of the cells within the white squares stained with Cnn (top, green in the merged picture) and Plp (middle, red in the merged picture). Scale bar, 10 μm.

(E) A dot-plot chart showing the quantification of Cnn fluorescence intensity at the centrosome in WT and Moe^{G0323} (n = 43 and n = 39 cells from eight WDs) during mitosis. The line represents the mean and the error bars the SD. SS was assessed by an unpaired Student's t test, **p < 0.010 and ****p < 0.0001.

(F) A comparative model of the behavior of extra centrosomes. In neuroblasts centrosomes (pink circles), all centrosomes are actively nucleating microtubules at prophase. During prometaphase, extra centrosomes cluster at the poles of the spindle. Un-clustered centrosomes remain randomly positioned in the cytoplasm and lose MT nucleation capacity (they become inactivated, yellow dot). In epithelial WDs, the frequently un-clustered centrosomes maintain MT nucleation capacity due to the presence of Moesin (red) at the centrosome. This leads to prolonged mitotic arrest and abnormal cell division.

See also Figure S5.

recruitment was perturbed in *SakOE* cells. However, quantification of Moe levels at the cortex did not show significant differences between WT and *SakOE* wing discs (Figure S4). Moreover, we did not notice any cortical phenotype as actin recruitment and mitotic rounding up were similar to WT cells (data not shown).

Interestingly, while characterizing Moe localization, we noticed that it was also localizing to centrosomes during prometaphase and metaphase (Figure 7A) while, by anaphase, Moe levels appeared reduced at the centrosome. In some cells, Moe was even associated with spindle MTs during metaphase (Figure 7A). Localization of Moe to the mitotic spindle has been described in S2 cells and *Drosophila* embryos [37], but not to the centrosomes. In addition, we found Moe enriched in centrosome-purified embryonic extracts (Figure 7B). Importantly, using the same imaging conditions, we did not detect Moe at the centrosome in neuroblasts even if it was associated with the cortex in these large non-epithelial cells (Figure 7C). However, Moe could be occasionally detected at centrosomes in neuroblasts if we increased the laser intensity, suggesting that Moe levels, at the centrosome, are highly reduced in these cells.

We next analyzed *SakOE* discs. In prometaphase Moe could be detected already in some, but not all, centrosomes. In metaphases and anaphase, Moe was localized to all centrosomes independently of whether they were clustered or un-clustered. Moreover, active centrosomes (associated with MT foci) always contained Moe (Figure 7A) even in anaphase, contributing to abnormal chromosome segregation.

We then analyzed the consequences of lowering Moe levels in PCM recruitment using a strong hypomorphic mutation, Moe^{G0323}. As described previously, low Moe levels resulted in the formation of bipolar spindles that showed defects in spindle positioning [26]. Importantly, characterization of Moe^{G0323} showed a clear defect in Cnn recruitment or maintenance in about 50% of mitotic cells (data not shown). Interestingly, an improvement of certain centrosomes during metaphase could be seen (Figure 7D). To better characterize this defect, we imaged wing discs expressing Cnn-RFP. Cnn is the major PCM component in *Drosophila* and plays essential roles in mitotic centrosome MT nucleation [38, 39]. In WT discs, Cnn-RFP was recruited in the beginning of mitosis, and its levels increased during prometaphase and metaphase, starting to decrease at anaphase (Figure S5). A similar behavior was also observed in about 50% of Moe^{G0323} cells. In this case, however, mitosis started with low levels of Cnn at the centrosome, but, during mitosis, a recovery in Cnn recruitment could be seen. In the remaining cells, Cnn levels were extremely low at the centrosome, and they never reached the levels observed in other mutant cells. These results strongly suggest a previously unknown role for Moe in Cnn recruitment.

Altogether, our study proposes that Moesin plays an essential role in influencing extra-centrosome behavior.

DISCUSSION

Here, we present an in vivo study of the consequences of centrosome amplification in the *Drosophila* wing disc. Our results uncovered different tissue related responses to centrosome amplification during mitosis. In addition, we provide a mechanistic insight into the observed differences. We show that in epithelial wing disc cells with extra centrosomes, centrosome inactivation also plays a major role in spindle bipolarization. Nevertheless, neither clustering nor inactivation is fully efficient and abnormal chromosome segregation was observed.

The same genetic background can have different consequences, at the same developmental stage in different tissues. To shed light on the reasons behind these discrepancies, we investigated protein content in wing discs and brains with extra centrosomes. We found that Moe, the only ERM member in flies, was specifically upregulated in *Sak*OE epithelial cells. A role for Moesin in spindle morphogenesis has been described in the past, but a role in PCM recruitment and therefore in spindle formation in WT cells or, in addition, in clustering and inactivation in cells with extra centrosomes, has never been reported. We found that Moe associates with mitotic centrosomes in the wing disc epithelia, and promotes, or maintains, MT nucleation of un-clustered centrosomes. Interestingly, Moe^{mut} display decreased PCM content. Importantly, while increased Moe levels sustains maintenance of MT nucleation activity from un-clustered centrosomes, reduction of Moe levels favors clustering of extra centrosomes. Recently, Moe was described as a cortical MAP with important functions in the stabilization of MTs at the cortex [40]. It is possible that this stabilization inhibits or delays clustering. Alternatively, a decrease in PCM content might also favor clustering. Our results are in agreement with these and extend our knowledge of Moesin versatility, opening new questions regarding the functions of the ERM protein family.

It remains to be explained why Moe levels are upregulated, in the presence of extra centrosomes, exclusively in *SakOE* wing discs, but not in *SakOE* brains. It is possible that Moe association with mitotic centrosomes and MTs is physiologically more important in epithelial cells, to promote timely and correct bipolar spindle formation. This advantage in cells that contain two centrosomes would become deleterious in cells with extra centrosomes. Importantly, the closely related ERM protein Merlin/NF2 plays an important function in clustering of extra centrosomes through restriction of Ezrin to the cell cortex in cancer cells [41]. Together, this shows how important ERM and Merlin family members are in regulating both actin and MT cytoskeletons.

Our work shows that, in epithelia, centrosome amplification is a tumor-initiating event. This is also the case in fly neuroblasts, but for different reasons.

Importantly, the effects of centrosome amplification, a common trait of carcinomas, are enhanced by higher levels of Moesin. Moesin is highly expressed in aggressive basal type breast carcinomas, it is transcriptionally upregulated upon EMT induction in breast cancer cell lines, and it is concomitant to the appearance of invasiveness markers, being a poor outcome prognostic marker [42–44].

SUPPLEMENTAL INFORMATION

Supplemental Information includes Supplemental Experimental Procedures and five figures and can be found with this article online at http://dx.doi.org/10.1016/j.cub.2015.01.066.

AUTHOR CONTRIBUTIONS

D.S. and R.B conceived the project, analyzed the data, and wrote the manuscript. D.S. did most of the experimental procedures, and D. Gogendeau set up the SILAC experiments and performed the SILAC experiments including data analysis and the centrosome purifications. D. Gambarotto performed the wing disc transplantation assays and part of the mitotic characterization. M.N. participated in the FISH experiments, and F.D. and D.L. performed the mass spec, and G.A. performed the statistical analysis. C.P. generated tools and performed the CP western blots. R.B. supervised the project.

ACKNOWLEDGMENTS

We thank B. Baum, R. Karess, J. Raff, C. Lehner, and F. Payre for reagents; L. Dumont, P. Tran, B. Baum, D. Lallemand, S. Godinho, M. Rujano, V. Marthiens, and Z. Storchova for helpful discussions and comments on the manuscript; L. Sengmanivong and F. Waharte for assistance at the Nikon imaging platform; and the Bloomington Stock Center and the Developmental Studies Hybridoma Bank University of Iowa for reagents. This work was supported by ERC starting grant (Centrostemcancer 242598), Institut Curie, CNRS, an FRM installation grant, ATIP grant and La Ligue contre le Cancer (M.N.). Our lab is a member of the CelTisPhyBio labex.

Received: September 23, 2014
Revised: December 22, 2014
Accepted: January 27, 2015
Published: March 12, 2015

REFERENCES

1. Kellogg, D.R., Moritz, M., and Alberts, B.M. (1994). The centrosome and cellular organization. Annu. Rev. Biochem. *63*, 639–674.
2. Bornens, M. (2002). Centrosome composition and microtubule anchoring mechanisms. Curr. Opin. Cell Biol. *14*, 25–34.
3. Nigg, E.A. (2006). Origins and consequences of centrosome aberrations in human cancers. Int. J. Cancer *119*, 2717–2723.
4. Zyss, D., and Gergely, F. (2009). Centrosome function in cancer: guilty or innocent? Trends Cell Biol. *19*, 334–346.
5. Kwon, M., Godinho, S.A., Chandhok, N.S., Ganem, N.J., Azioune, A., Thery, M., and Pellman, D. (2008). Mechanisms to suppress multipolar divisions in cancer cells with extra centrosomes. Genes Dev. *22*, 2189–2203.
6. Basto, R., Brunk, K., Vinadogrova, T., Peel, N., Franz, A., Khodjakov, A., and Raff, J.W. (2008). Centrosome amplification can initiate tumorigenesis in flies. Cell *133*, 1032–1042.
7. Ganem, N.J., Godinho, S.A., and Pellman, D. (2009). A mechanism linking extra centrosomes to chromosomal instability. Nature *460*, 278–282.
8. Leber, B., Maier, B., Fuchs, F., Chi, J., Riffel, P., Anderhub, S., Wagner, L., Ho, A.D., Salisbury, J.L., Boutros, M., and Krämer, A. (2010). Proteins required for centrosome clustering in cancer cells. Sci. Transl. Med. *2*, 33ra38.
9. Marthiens, V., Rujano, M.A., Pennetier, C., Tessier, S., Paul-Gilloteaux, P., and Basto, R. (2013). Centrosome amplification causes microcephaly. Nat. Cell Biol. *15*, 731–740.
10. Habedanck, R., Stierhof, Y.D., Wilkinson, C.J., and Nigg, E.A. (2005). The Polo kinase Plk4 functions in centriole duplication. Nat. Cell Biol. *7*, 1140–1146.
11. Bettencourt-Dias, M., Rodrigues-Martins, A., Carpenter, L., Riparbelli, M., Lehmann, L., Gatt, M.K., Carmo, N., Balloux, F., Callaini, G., and Glover, D.M. (2005). SAK/PLK4 is required for centriole duplication and flagella development. Curr. Biol. *15*, 2199–2207.
12. Kleylein-Sohn, J., Westendorf, J., Le Clech, M., Habedanck, R., Stierhof, Y.D., and Nigg, E.A. (2007). Plk4-induced centriole biogenesis in human cells. Dev. Cell *13*, 190–202.
13. Weinberg, R.A. (2006). The Biology of Cancer. (New York: Garland).
14. Lee, H.S., Simon, J.A., and Lis, J.T. (1988). Structure and expression of ubiquitin genes of Drosophila melanogaster. Mol. Cell. Biol. *8*, 4727–4735.
15. Adler, P.N., and MacQueen, M. (1984). Cell proliferation and DNA replication in the imaginal wing disc of Drosophila melanogaster. Dev. Biol. *103*, 28–37.
16. Martinez-Campos, M., Basto, R., Baker, J., Kernan, M., and Raff, J.W. (2004). The Drosophila pericentrin-like protein is essential for cilia/flagella function, but appears to be dispensable for mitosis. J. Cell Biol. *165*, 673–683.
17. Silkworth, W.T., Nardi, I.K., Scholl, L.M., and Cimini, D. (2009). Multipolar spindle pole coalescence is a major source of kinetochore mis-attachment and chromosome mis-segregation in cancer cells. PLoS ONE *4*, e6564.
18. Silkworth, W.T., and Cimini, D. (2012). Transient defects of mitotic spindle geometry and chromosome segregation errors. Cell Div. *7*, 19.
19. Pandey, R., Heeger, S., and Lehner, C.F. (2007). Rapid effects of acute anoxia on spindle kinetochore interactions activate the mitotic spindle checkpoint. J. Cell Sci. *120*, 2807–2818.
20. Schittenhelm, R.B., Heeger, S., Althoff, F., Walter, A., Heidmann, S., Mechtler, K., and Lehner, C.F. (2007). Spatial organization of a ubiquitous eukaryotic kinetochore protein network in Drosophila chromosomes. Chromosoma *116*, 385–402.
21. Thompson, S.L., and Compton, D.A. (2010). Proliferation of aneuploid human cells is limited by a p53-dependent mechanism. J. Cell Biol. *188*, 369–381.
22. Holland, A.J., and Cleveland, D.W. (2012). Losing balance: the origin and impact of aneuploidy in cancer. EMBO Rep. *13*, 501–514.
23. Pfau, S.J., and Amon, A. (2012). Chromosomal instability and aneuploidy in cancer: from yeast to man. EMBO Rep. *13*, 515–527.
24. Dekanty, A., Barrio, L., Muzzopappa, M., Auer, H., and Milán, M. (2012). Aneuploidy-induced delaminating cells drive tumorigenesis in Drosophila epithelia. Proc. Natl. Acad. Sci. USA *109*, 20549–20554.
25. Guilgur, L.G., Prudêncio, P., Ferreira, T., Pimenta-Marques, A.R., and Martinho, R.G. (2012). Drosophila aPKC is required for mitotic spindle orientation during symmetric division of epithelial cells. Development *139*, 503–513.
26. Nakajima, Y., Meyer, E.J., Kroesen, A., McKinney, S.A., and Gibson, M.C. (2013). Epithelial junctions maintain tissue architecture by directing planar spindle orientation. Nature *500*, 359–362.
27. Poulton, J.S., Cuningham, J.C., and Peifer, M. (2014). Acentrosomal Drosophila epithelial cells exhibit abnormal cell division, leading to cell death and compensatory proliferation. Dev. Cell *30*, 731–745.
28. D'Avino, P.P., Savoian, M.S., and Glover, D.M. (2005). Cleavage furrow formation and ingression during animal cytokinesis: a microtubule legacy. J. Cell Sci. *118*, 1549–1558.
29. Gisselsson, D., Jin, Y., Lindgren, D., Persson, J., Gisselsson, L., Hanks, S., Sehic, D., Mengelbier, L.H., Øra, I., Rahman, N., et al. (2010). Generation of trisomies in cancer cells by multipolar mitosis and incomplete cytokinesis. Proc. Natl. Acad. Sci. USA *107*, 20489–20493.
30. Caussinus, E., and Gonzalez, C. (2005). Induction of tumor growth by altered stem-cell asymmetric division in Drosophila melanogaster. Nat. Genet. *37*, 1125–1129.
31. Morais da Silva, S., Moutinho-Santos, T., and Sunkel, C.E. (2013). A tumor suppressor role of the Bub3 spindle checkpoint protein after apoptosis inhibition. J. Cell Biol. *201*, 385–393.
32. Gonzalez, C. (2013). Drosophila melanogaster: a model and a tool to investigate malignancy and identify new therapeutics. Nat. Rev. Cancer *13*, 172–183.
33. Uhlirova, M., and Bohmann, D. (2006). JNK- and Fos-regulated Mmp1 expression cooperates with Ras to induce invasive tumors in Drosophila. EMBO J. *25*, 5294–5304.
34. Polesello, C., and Payre, F. (2004). Small is beautiful: what flies tell us about ERM protein function in development. Trends Cell Biol. *14*, 294–302.

35. Kunda, P., and Baum, B. (2009). The actin cytoskeleton in spindle assembly and positioning. Trends Cell Biol. *19*, 174–179.

36. Kunda, P., Pelling, A.E., Liu, T., and Baum, B. (2008). Moesin controls cortical rigidity, cell rounding, and spindle morphogenesis during mitosis. Curr. Biol. *18*, 91–101.

37. Vilmos, P., Jankovics, F., Szathmári, M., Lukácsovich, T., Henn, L., and Erdélyi, M. (2009). Live imaging reveals that the Drosophila actin-binding ERM protein, moesin, co-localizes with the mitotic spindle. Eur. J. Cell Biol. *88*, 609–619.

38. Lucas, E.P., and Raff, J.W. (2007). Maintaining the proper connection between the centrioles and the pericentriolar matrix requires Drosophila centrosomin. J. Cell Biol. *178*, 725–732.

39. Conduit, P.T., Feng, Z., Richens, J.H., Baumbach, J., Wainman, A., Bakshi, S.D., Dobbelaere, J., Johnson, S., Lea, S.M., and Raff, J.W. (2014). The centrosome-specific phosphorylation of Cnn by Polo/Plk1 drives Cnn scaffold assembly and centrosome maturation. Dev. Cell *28*, 659–669.

40. Solinet, S., Mahmud, K., Stewman, S.F., Ben El Kadhi, K., Decelle, B., Talje, L., Ma, A., Kwok, B.H., and Carreno, S. (2013). The actin-binding ERM protein Moesin binds to and stabilizes microtubules at the cell cortex. J. Cell Biol. *202*, 251–260.

41. Hebert, A.M., DuBoff, B., Casaletto, J.B., Gladden, A.B., and McClatchey, A.I. (2012). Merlin/ERM proteins establish cortical asymmetry and centrosome position. Genes Dev. *26*, 2709–2723.

42. Haynes, J., Srivastava, J., Madson, N., Wittmann, T., and Barber, D.L. (2011). Dynamic actin remodeling during epithelial-mesenchymal transition depends on increased moesin expression. Mol. Biol. Cell *22*, 4750–4764.

43. Charafe-Jauffret, E., Monville, F., Bertucci, F., Esterni, B., Ginestier, C., Finetti, P., Cervera, N., Geneix, J., Hassanein, M., Rabayrol, L., et al. (2007). Moesin expression is a marker of basal breast carcinomas. Int. J. Cancer *121*, 1779–1785.

44. Wang, C.C., Liau, J.Y., Lu, Y.S., Chen, J.W., Yao, Y.T., and Lien, H.C. (2012). Differential expression of moesin in breast cancers and its implication in epithelial-mesenchymal transition. Histopathology *61*, 78–87.